Tetrahedron 72 (2016) 4637–4642

Contents lists available at ScienceDirect

Tetrahedron

journal homepage: www.elsevier.com/locate/tet

A new ratiometric two-photon fluorescent probe for imaging of lysosomes in living cells and tissues

Liyi Zhou [a,b,c,*], Yongchao Liu [b], Shunqin Hu [a], Haifei Wang [a], Hongyan Sun [c], Xiaobing Zhang [b]

[a] College of Packaging and Materials Engineering, Hunan University of Technology, Hunan 412007, PR China
[b] Molecular Sciences and Biomedicine Laboratory, State Key Laboratory for Chemo/Biosensing and Chemometrics, College of Chemistry and Chemical Engineering, Collaborative Innovation Center for Chemistry and Molecular Medicine, Hunan University, Changsha 410082, PR China
[c] Department of Biology and Chemistry, City University of Hong Kong, 83 Tat Chee Avenue, Kowloon, Hong Kong, PR China

ARTICLE INFO

Article history:
Received 2 April 2016
Received in revised form 19 May 2016
Accepted 12 June 2016
Available online 18 June 2016

Keywords:
Two-photon
Ratiometric fluorescent probe
Lysosomal pH
Fluorescent imaging

ABSTRACT

Intracellular pH plays a pivotal role in various biological processes. Herein, we adopted the through bond energy transfer (TBET) strategy to design a unique type of ratiometric two-photon fluorescent probe for imaging of lysosomal pH in live cells and tissues, termed Np-Rh-Lys. Specifically, a two-photon fluorophore (D-π-A-structured naphthalimide derivative) and a rhodamine B fluorophore were directly connected, and dimethylamino moiety served as a lysosomal targeting-group. The experiments demonstrate new probe Np-Rh-Lys was a reliable and specific probe for labeling lysosomes in living cells with two well-resolved emission peaks separated by 80 nm, and which showed high ratiometric imaging resolution and deep-tissue imaging depth over 180 μm, we thus may expect the new platform prompt the development of a wide variety of ratiometric two-photon fluorescent probes application in biological systems.

1. Introduction

In living cells, lysosome is the major subcellular organelles. Lysosome contains numerous enzymes and proteins exhibiting a variety of activities and functions at pH values (4.5–5.5).[1] In order to maintain the lysosomal pH values, the protons are pumped into lysosomal interior by a membrane-bound ATPase. Importantly, the cellular apoptosis process associates with the gradient decay of lysosomal proton, which leads to the increase of the lysosomal pH values.[2–4] Once, the dysfunction of lysosomes are induced various pathologies including neurodegenerative diseases,[5] cancer,[6] and Alzheimer's disease.[7,8] Wherefore, it is important to monitor the lysosomal pH values changes in living cells and tissues.

Fluorescent imaging is coming into widespread use in various analytes in living cells, tissues and organisms by virtue of their high sensitivity, high-speed spatial analysis, and less bio-damaging. Traditionally, chemical probes for detecting targeting analytes in an organelle are rationally designed by incorporating an organelle-specific moiety as the guiding moiety. For example, positive cation functional moieties were used for targeting mitochondria and weakly alkaline functional moieties were used for targeting lysosome.[9–12] To image and track the acidic vesicles in living cells, two main classes of pH-sensitive fluorescent probes have been developed. The first category was turn-on probe based on a photo-induced electron transfer (PET) system.[13–15] The second category was the ratiometric probe based on spectral shift in the emission during proton binding.[16] Of these two types of probes, the ratiometric probes have been mostly used for quantitative analysis, because a turn-on response within a single detection window can vary depending on the experimental conditions such as incident laser power and probe distribution. Ratiometric probes, on the other hand, can eliminate these interferences by the built-in correction of the dual emission bands, resulting in a more favorable system for imaging living systems. However, most of these fluorescent probes were used one-photon-excited and emit at a short wavelength in the visible region, which resulted in some obvious drawbacks for bioimaging, such as photobleaching, high auto-fluorescence background and shallow penetration depth. Therefore, it is of great significance and necessity to develop simple and reliable fluorescent probe for quantitative measurement of lysosomal pH values changes in live cells and tissues.

To solve these problems, an effective tool is two-photon fluorescence microscopy (TPFM). In this paper, based on the

* Corresponding author. Tel./fax: +86 18711056980; e-mail address: zhouly0817@163.com (L. Zhou).

http://dx.doi.org/10.1016/j.tet.2016.06.038
0040-4020/

previously works,[17] we have established a new ratiometric two-photon fluorescent probe Np-Rh-Lys, by directly connect a two-photon D-π-A-structure naphthalimide derivative with a rhodamine B fluorophore via the through bond energy transfer (TBET) strategy. The probe molecule exhibited a highly efficient energy transfer with two well-resolved emission peaks, which afford a high sensitivity for the H^+-response, and high resolution observed for H^+ ions. It showed a pronounced fluorescent response toward H^+ ions over other common metal ions and neuter moleculars. The probe was then used for TPFM imaging of pH in live cancer cells and plant cells, showed high ratiometric imaging resolution and large tissue-imaging depth. The synthesis processes and the all structural characterization (using ^1H NMR, ^{13}C NMR, and MS) are provided in the Scheme 1 and the Supplementary data, respectively.

imaging to develop a TBET-based ratiometric two-photon fluorescent probe. As a proof of principle, D-π-A-structured naphthalimide derivative was chosen as a donor for its excellent two-photon properties, while rhodamine B was selected as an acceptor for its target-triggered 'turn-on' fluorescent signal that can be easily distinguished, and alkaline dimethylamino served as a lysosomal targeting-group. This type of TBET-based ratiometric two-photon fluorescent probe, termed Np-Rh-Lys (Scheme 1). The structure of Np-Rh-Lys was characterized by ^1H NMR, ^{13}C NMR, and MS (See the Supplementary data) (see Fig. 1).

2.2. Optical property and selectivity of Np-Rh-Lys

The spectroscopic properties of Np-Rh-Lys was examined in 10 mM phosphate buffer solution (PBS) of different pH values. The

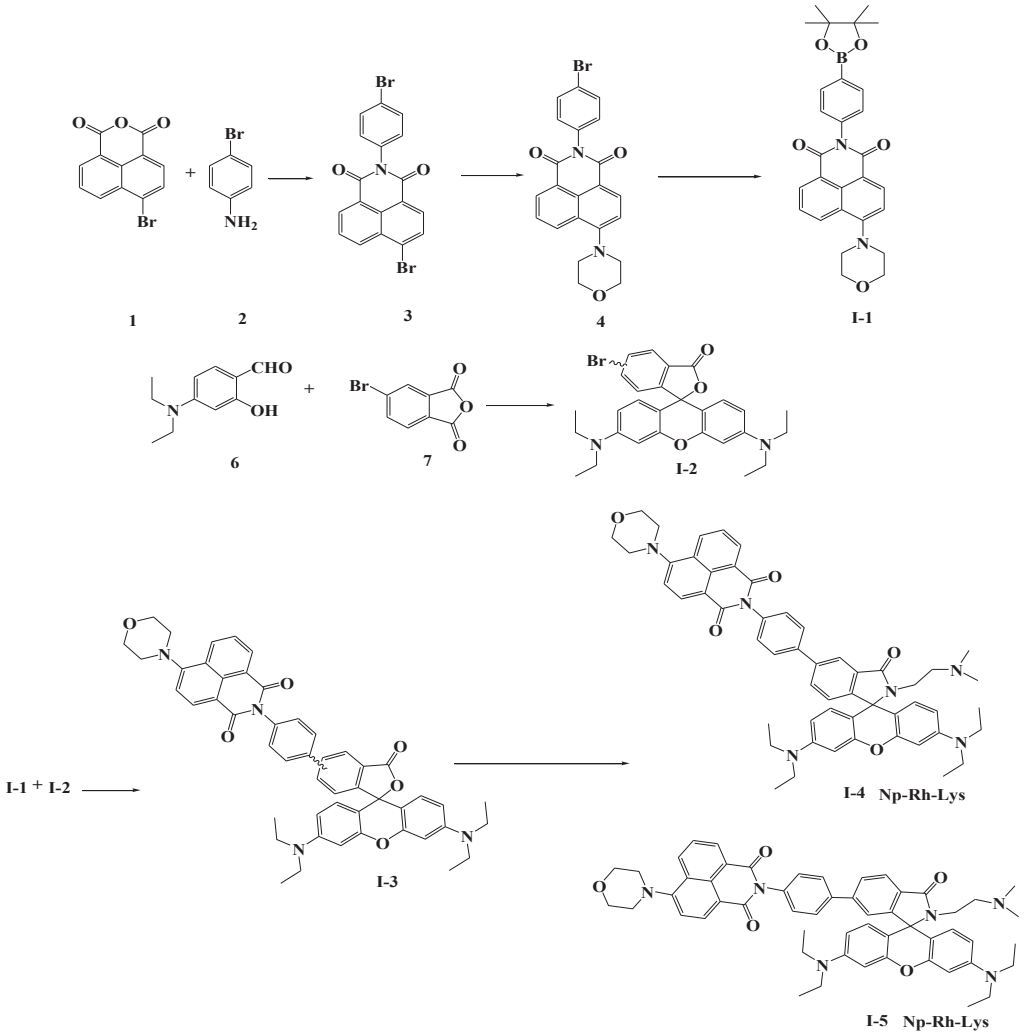

Scheme 1. The synthetic route of the probe Np-Rh-Lys.

2. Results and discussion

2.1. Design and synthesis of compounds Np-Rh-Lys

The two-photon fluorescent activity of D-π-A-structured naphthalimide derivatives have been reported.[18,19] In order to acquire the better bioimaging results, we decided to combine the advantages of two-photon fluorescent imaging and the ratiometric

probe displayed different absorption (Fig. 2B) and fluorescent (Fig. 2A) spectra with different pH values. As shown in Fig. 2B, the probe exhibited a maximum absorption band at 400 nm at pH 7.4, which belonged to the donor moiety. What's more, at pH 3.0, it showed two maximum absorption bands at 400 and 550 nm, respectively, which belonged to the donor moiety and the spirocyclization opened form of the xanthene unit (acceptor moiety). Meanwhile, the probe solution' color changed from green to red

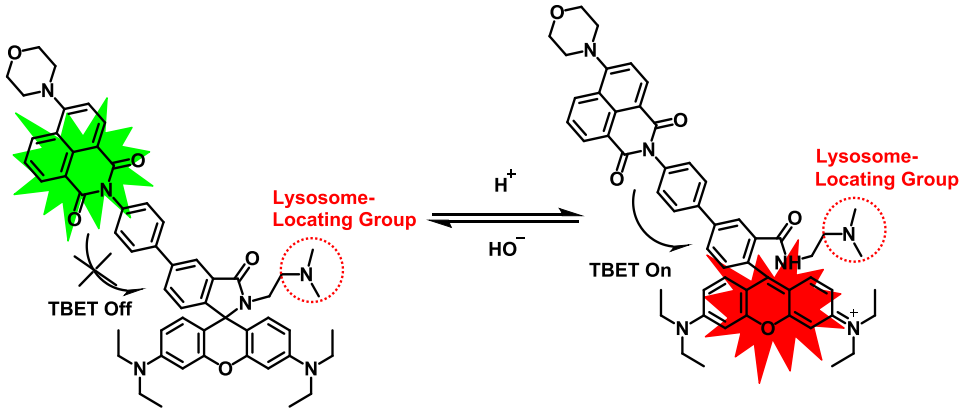

Fig. 1. Structure of Np-Rh-Lys and its response mechanism to pH or lysosomal pH.

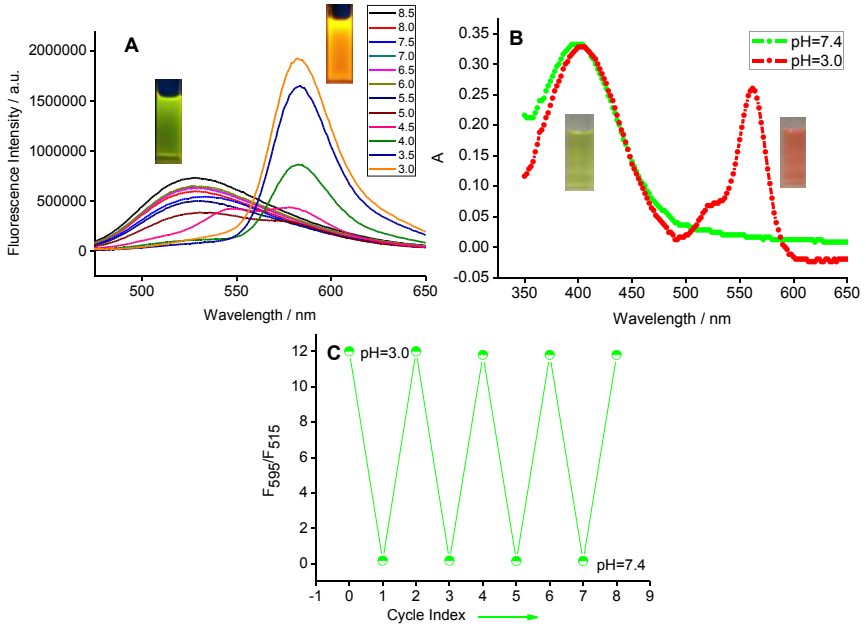

Fig. 2. (A) Fluorescence emission spectra of Np-Rh-Lys (1 μM) in PBS buffer (10 mM) at different pH values; (B) UV-Absorption spectra of probe Np-Rh-Lys (1 μM) under pH value 3.0 and 7.4, respectively; (C) pH reversibility study of Np-Rh-Lys between pH 3.0 and 7.4, λ_{ex}=400 nm.

was observed with pH value between 7.4 and 3.0 (see Fig. 2B). Once upon excitation at 400 nm, the fluorescent emission intensity of Np-Rh-Lys at 595 nm decreases significantly with the pH values from 3.0 to 7.4, accompanying with a large increase of fluorescence intensity at 515 nm (Fig. 2A), which provided the basis to achieve a ratiometric (F_{515}/F_{595}) detection and imaging of pH. The probe also showed a good reversibility between pH 3.0 and pH 7.4 (Fig. 2C), which was attributed to the reversible spirocyclization opened/closed form of the probe molecule (Fig. 2). These results indicated that the ratiometric response of Np-Rh-Lys matched well with the physiological pH value range (pH 4.5–5.0) of lysosomes, making it promising as a ratiometric fluorescent probe for accurate measurement of lysosomal pH values.

Selectivity is an important parameter to evaluate the performance of a new fluorescent probe. Particularly, for a bio-imaging probe with potential application in complex biological samples, a highly selective response to the target species over other potentially competing kinds is necessary. As shown in Fig. S1 (see Supplementary data), the selectivity experiments showed that various anions, cations and thiol amino acids have no interference on the fluorescent response of Np-Rh-Lys to pH. Wherefore, Np-Rh-Lys could be applied in living cells to track pH value of the acidic vesicles.

2.3. Colocalization and ratiometric two-photon imaging in living cells

In order to evaluate the imaging performance of ratiometric probe Np-Rh-Lys in vivo, the HeLa cells were chosen as the model cell line. At first, the cytotoxic effects of Np-Rh-Lys were assessed using the MTT assay. The results indicated that the Np-Rh-Lys was nearly nontoxic to live cells under experimental conditions, the IC50 was 28.2 μM (Supplementary data, Fig. S2). Following test, the HeLa cells were co-stained with Np-Rh-Lys and LysoSensor blue which is a commercially available lysosome-specific staining probe. As shown in Fig. 3a–d, the confocal fluorescence microscopy results showed that Np-Rh-Lys overlayed well with LysoSensor blue, which reveals that Np-Rh-Lys can selectively stain lysosomes in live cells, and the ratiometric two-photon images exhibited with high resolution between the green and the red channels (Fig. 3e–h).

2.4. Tissues slice ratiometric imaging

At last, Np-Rh-Lys was used for onion tissue cells ratiometric imaging. The changes of fluorescence signal intensity with scan

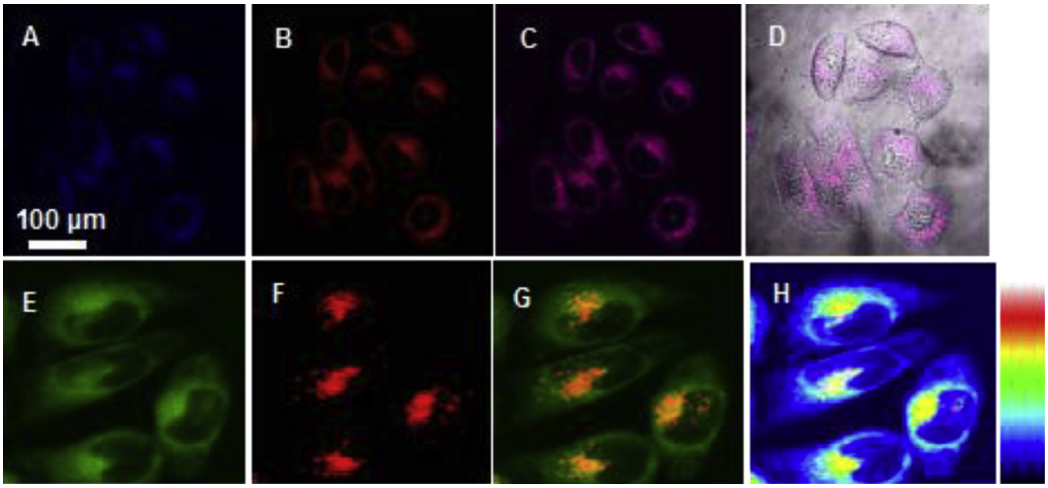

Fig. 3. Colocalization images and two-photon ratiometric images of HeLa cells. (A) Colocalization regent lysosome-blue (1 μM, blue channel, λ_{ex}=405 nm, λ=415–455 nm). (B) Np-Rh-Lys (1 μM, red channel, λ_{ex}=559 nm, λ_{em}=560–650 nm). (C) overlay imaging of (A) and (B). (D) overlay imaging of (A), (B) and bright field imaging. (E) Two-photon of green channel images. (F) Two-photon of red channel images. (G) overlay imaging of (E) and (F). (H) pseudo color imaging of (E), (F) and (G) Scale bar: 100 μm, $\lambda_{two\text{-}photon\ ex}$=780 nm, one-photon and two-photon images were acquired with a 60×oil or 100×oil immersion objective, respectively.

depth were determined by spectral confocal multiphoton microscopy (Olympus, FV1000) in the z-scan mode. Depth scanning demonstrated that the corresponding Np-Rh-Lys product was capable of tissue cells imaging at depths of 40–180 μm by TPFM imaging, the results were presented in two emission channels with different colors (see Fig. 4 and Fig. S3 in Supplementary data). These data showed that Np-Rh-Lys possessed good tissue penetration, high resolution, staining ability, and it was also used for lysosomal pH ratiometric imaging in the plant cells, as well as ratiometric two-color (green and red) imaging changes.

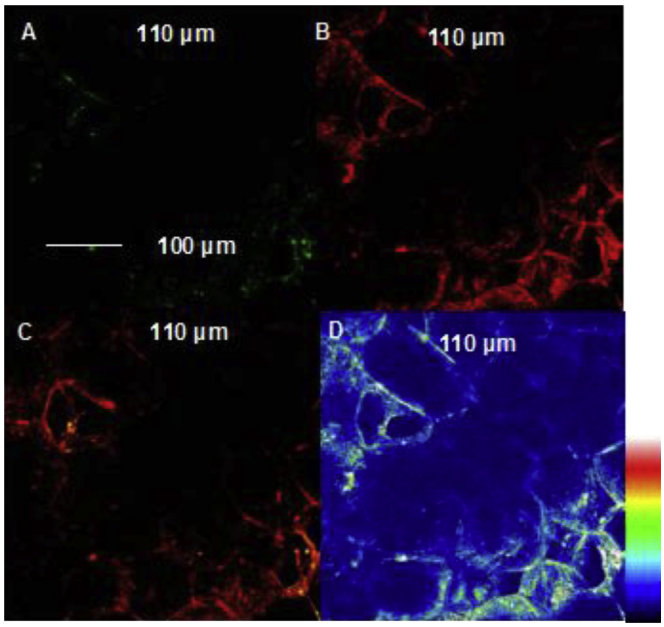

Fig. 4. TPFM of an onion epidermal tissue slice ratiometric imaging. (A) and (B) stained with 5 μM Np-Rh-Lys at 110 μm for 60 min. (C) The imagings overlayed (A) and (B). (D) Ratiometric imaging of (A) and (B). The images were collected at 470–530 nm (green channel, A) and 550–650 nm (red channel, B) upon excitation at 780 nm with femtosecond pulses. Scale bars: 100 μm.

3. Conclusion

In summary, we have developed a new lysosome-targeting ratiometric two-photon fluorescent probe (Np-Rh-Lys) by hybridizing a weakly alkaline dimethylamine moiety with an xanthane derivative and a two-photon naphthalimide fluorophore. The xanthane derivative of the probe exhibits a pH-modulated open/close reaction of the spirocycle, while the two-photon naphthalimide moiety as an internal standard, which affords the probe a ratiometric fluorescence response towards pH. Confocal microscopic images of HeLa cells labeled with Np-Rh-Lys revealed two distinct emission ranges at 485–530 nm (green) and 560–610 nm (red) in living cells. Colocalization experiments confirmed that the fluorescence of probe Np-Rh-Lys overlayed with a lysosome-specific staining dye, demonstrated its strong lysosomal localization capability. The probe can be readily prepared and shows lysosome-targeting ability, high resolution and low cytotoxicity. More importantly, we successfully used the ratiometric two-photon probe Np-Rh-Lys to monitor the pH in live animal cells and plant cells. We believe that Np-Rh-Lys could be widely applied in biological systems imaging.

4. Experimental

4.1. Materials and instruments

Unless otherwise specified, all chemicals were obtained from commercial suppliers and used without further purification. Thin layer chromatography (TLC) was carried out using silica gel F254, and column chromatography was conducted over silica gel (100–200 mesh), both of them were obtained from Qingdao Ocean Chemicals (Qingdao, China). In all experiments, water used was doubly distilled and purified by a Milli-Q system (Millipore, USA). LC-MS analyses were performed using an Agilent 1100 HPLC/MSD spectrometer. Mass spectra were performed using an LCQ Advantage ion trap mass spectrometer (Thermo Finnigan). ^{1}H NMR and ^{13}C NMR spectra were obtained using a Bruker DRX-400 spectrometer using TMS as an internal standard. All chemical shifts are reported in the standard δ notation of parts per million. UV–vis absorption spectra were recorded in 1.0 cm path length quartz cuvettes on a Shimadzu 2450 UV-visible Spectrometer. HeLa cells

and onion tissues were obtained from the College of Biological Sciences of Hunan University, and the fluorescence images of HeLa cells and onion tissues were obtained using Olympus FV1000-MPE multiphoton laser scanning confocal microscope (Japan). Fluorescence measurements were carried out on a F4500 fluorescence spectrometer with excitation and emission slits set at 5.0 nm and 5.0 nm, respectively. The pH was measured with a Mettler-Toledo Delta 320 pH meter.

4.2. Synthesis of compounds 3, 6, 7, and Np-Rh-Lys

Synthesis of compound **3**: compound **1** (0.01 mol, 2.57 g) and compound **2** (0.011 mol, 1.8 g) were dissolved in glacial acetic acid (100 mL). The mixture was heated to reflux for 4 h, then poured into 250 mL ice-water, the solid was washed with $HCl_{(aq)}$ (1.0 mol/L) and $NaOH_{(aq)}$ (1.0 mol/L), respectively, and then the gray white solid was obtained via the vacuum pump leak and dried under the vacuum oven. ^{1}H NMR (400 MHz, DMSO-d_6) δ_H: 10.07 (s, 1H), 8.63–8.59 (t, J=4 Hz, 1H), 8.35–8.26 (t, J=18 Hz, 1H), 8.03 (s, 1H), 7.76–7.74 (d, J=4 Hz, 1H),7.56–7.54 (d, J=4 Hz, 1H), 7.48–7.39 (m, 4H).

Synthesis of compound **4**: Compound **3** (0.0046 mol, 2.0 g) and morpholine (20 mL, excess) were added together, and then heated to reflux for 8 h, the mixture was cooled to room temperature, and then poured into 200 mL ice-water, and then, the yellow solid was obtained through filtration and dried by the vacuum oven. ^{1}H NMR (400 MHz, DMSO-d_6) δ_H: 8.65–8.64 (d, J=2 Hz, 1H), 8.63–8.60 (d, J=6 Hz, 1H), 8.58–8.51 (d, J=14 Hz, 1H), 7.74–7.66 (m, 3H), 7.29–7.19 (m, 3H), 4.07–4.04 (t, J=6 Hz, 4H), 3.33–3.30 (t, J=6 Hz, 4H). +C ESI ms=434.3, calcd=436.1.

Synthesis of the **I-1**, **I-2**, and **I-3** was followed the reference.[17] These compounds only used the ms to be proved without further purification, and directly to do the next steps. +C ESI ms for **I-1**=485.3, **I-2**=521.3, **I-3**=799.5.

Synthesis of the Np-Rh-Lys: **I-3** (0.63 mmol, 0.5 g), ethanol 50 mL, and 2-dimethylaminoethylamine 5 mL were added together, to continue heating to reflux for another 4 h. The resulting mixture solution was rotary evaporated. The yellow solid **I-4/5** was obtained through column chromatography with petroleum ether/ethyl acetate=5:1 (v/v). Finally, we chose a larger polarity of compound for structural confirmation and testing. ^{1}H NMR (400 MHz, DMSO-d_6) δ_H: 8.55–8.37 (m, 3H), 7.89–7.86 (t, J=6 Hz, 2H), 7.84–7.79 (m, 1H), 7.69–7.67 (d, J=8 Hz, 1H), 7.49–7.47 (d, J=8 Hz, 1H), 7.39–7.34 (m, 3H), 6.41–6.39 (dd, J=4 Hz, 6H), 3.92–3.91 (d, J=4 Hz, 4H), 3.38 (s, 1H), 3.34–3.30 (t, J=8 Hz, 6H), 3.23 (s, 4H), 3.10–3.03 (m, 2H), 1.90 (s, 6H), 1.08–1.05 (t, J=6 Hz, 12H). ^{13}C NMR (400 MHz, DMSO-d_6) δ_C: 169.12, 161.19, 152.72, 152.54, 152.42, 149.62, 149.46, 135.71, 128.94, 126.85, 124.79, 124.35, 112.39, 108.76, 106.99, 105.12, 102.08, 97.17, 84.28, 48.71, 47.53, 44.56, 44.11, 12.63. +C ESI ms=869.5, calcd=869.4.

4.3. Spectrophotometric measurements

The fluorescence measurement experiments were measured in phosphate buffer solution (10 mM) with DMSO as co-solvent solution (H_2O/DMSO=99:1, v/v). The pH value of PBS solution used was from 3.0 to 7.4, which was achieved by adding minimal volumes of HCl solution or NaOH solution. The fluorescent emission spectra was recorded at excitation wavelength of 400 nm with emission wavelength range from 475 to 650 nm. A 1×10^{-3} mol/L stock solution of probe was prepared by dissolving probe compound in DMSO. Procedure of calibration measurements with probe in the buffer with different pH followed: 20 μL stock solution of probe and 1980 μL PBS buffer solution with different pH were combined to afford a test solution, which contained 1×10^{-6} mol/L of probe. The solutions of various testing species were prepared from NaCl, $CaCl_2$, $MgSO_2$, $CuCl_2\cdot H_2O$, $Zn(NO_3)_2\cdot 6H_2O$, using twice-distilled water with final concentrations of 0.0125 mol/L, as well as, glutathione (GSH), cysteine (Cys), and glutamate (Glu) using twice-distilled water with final concentrations of 0.025 mol/L. Procedure of selectivity experiments followed: for cations or anions, 20 μL stock solution of probe, 1948 μL PBS solution (pH 7.0) and 32 μL solution of each cation or anion were combined to afford a test solution, which contained 1×10^{-6} mol/L of probe and 200 μM cation or anion; for amino acids, 20 μL stock solution of probe, 1900 μL PBS buffer solution (pH 7.4) and 80 μL solution of each amino acid were combined to afford a test solution, which contained 1×10^{-6} mol/L of probe and 1 mmol/L amino acid.

4.4. Cell cytotoxic assays and imaging

The cytotoxic effects of probe were assessed using the MTT assay. The HeLa cells were treated with **Np-Rh-Lys** (0, 2.0, 4.0, 6.0, 8.0, 10.0, 20.0, 30.0, 40.0, 50.0, 60.0, 70.0, 80.0, 90.0, 100.0 μM), and then using the log([Np-Rh-Lys]/μM) as the x-axis and the cell viability as the y-axis, at last via the origin fitting with a standard curve and calculate the IC50. Before the cells imaging, the cells were washed with PBS buffered solution, followed by incubating with probe (1 μM) for 30 min (in PBS containing 1% DMSO) at 37 °C, then by washing with PBS three times and imaged. Lyso-Tracher blue (1 μM, Invitrogen) was used for co-staining experiments. The one-photon excitation wavelength was fixed at 405 nm and 535 nm. The fluorescent emissions wavelength were recorded at (425–475) nm, (495–540) nm and (560–650) nm, individually. The two-photon excitation wavelength was fixed at 780 nm.

4.5. Preparation and staining of plant tissue slice

The slices were cultured with 5 μM **Np-Rh-Lys** in an incubator at 37 °C for 1 h and then washed with PBS three times for TPFM imaging. The TPFM images (with a magnification at 10 times) were collected in two channels (green: 495–540 nm, and red: 560–650 nm) upon excitation at 780 nm with a pulse laser.

Acknowledgements

This work was supported by the National Key Scientific Program of China (2011CB911000), NSFC (Grants 21325520, 21327009, J1210040, 21177036), the Foundation for Innovative Research Groups of NSFC (Grant 21221003), the National Natural Science Foundation of China (21135001), the National Instrumentation Program (2011YQ030124), State Key Laboratory of Fine Chemicals Dalian University of Technology (KF1301) and the Hunan Provincial Natural Science Foundation (Grant 11JJ1002).

Supplementary data

Supplementary data related to this article can be found at http://dx.doi.org/10.1016/j.tet.2016.06.038.

References and notes

1. Kornfeld, S.; Mellman, I. *Annu. Rev. Cell Biol.* **1989**, *5*, 483–525.
2. Blott, E. J.; Griffiths, G. M. *Nat. Rev. Mol. Cell Biol.* **2002**, *3*, 122–131.
3. Stinchcombe, J.; Bossi, G.; Griffiths, G. M. *Science* **2004**, *305*, 55–59.
4. Nilsson, C.; Kagedal, K.; Johansson, U.; Öllinger, K. *Methods Cell Sci.* **2004**, *25*, 185–194.
5. Zhang, L.; Sheng, R.; Qin, Z. *Acta Biochim. Biophys. Sin.* **2009**, *41*, 437–445.
6. Schindler, M.; Grabski, S.; Hoff, E.; Simon, S. M. *Biochemistry* **1996**, *35*, 2811–2817.
7. Russell, D. A.; Pottier, R. H.; Valenzeno, D. P. *Photochem. Photobiol.* **1994**, *59*, 309–313.
8. Mogensen, H. S.; Beatty, D. M.; Morris, S. J.; Jorgensen, O. S. *Neuroreport* **1998**, *9*, 1553–1558.
9. Dickinson, B. C.; Srikun, D.; Chang, C. J. *Curr. Opin. Chem. Biol.* **2010**, *14*, 50–56.

10. Smith, R. A.; Hartley, R. C.; Murphy, M. P. *Antioxid. Redox Signal.* **2011**, *15*, 3021–3038.
11. Fan, J. L.; Dong, H. J.; Hu, M. M.; Wang, J. Y.; Zhang, H.; Zhu, H.; Peng, X. *Chem. Commun.* **2014**, 882–884.
12. Best, Q. A.; Xu, R. S.; McCarroll, M. E.; Wang, L. C.; Dyer, D. J. *Org. Lett.* **2010**, *12*, 3219–3221.
13. Zhu, H.; Fan, J. L.; Xu, Q. L.; Li, H. L.; Wang, J. Y.; Gao, P.; Peng, X. *Chem. Commun.* **2012**, 11766–11768.
14. Shi, X. L.; Mao, G. J.; Zhang, X. B.; Liu, H. W.; Gong, Y. J.; Wu, Y. X.; Zhou, L.; Tan, W. *Talanta* **2014**, *130*, 356–362.
15. Yang, S.; Qi, Y.; Liu, C. H.; Wang, Y. J.; Zhao, Y. R.; Wang, L. L.; Yang, R. H. *Anal. Chem.* **2014**, *86*, 7508–7515.
16. Wan, Q.; Chen, S.; Shi, W.; Li, L.; Ma, H. *Angew. Chem., Int. Ed.* **2014**, *53*, 10916–10920.
17. Zhou, L.; Zhang, X. B.; Wang, Q.; Lv, Y.; Mao, G.; Luo, A.; Zhang, J.; Tan, W. *J. Am. Chem. Soc.* **2014**, *136*, 9838–9841.
18. Qian, Y.; Xiao, Y.; Guo, X.; Qian, J.; Zhu, W. *Chem. Commun.* **2010**, 6418–6436.
19. Zhang, J. F.; Lim, C. S.; Bhuniya, S.; Cho, B. R.; Kim, J. S. *Org. Lett.* **2011**, *13*, 1190–1193.